PHYSICAL REVIEW B **75**, 060501(R) (2007)

Electronic structure of electron-doped $Sm_{1.86}Ce_{0.14}CuO_4$: Strong pseudogap effects, nodeless gap, and signatures of short-range order

S. R. Park,[1] Y. S. Roh,[1] Y. K. Yoon,[1] C. S. Leem,[1] J. H. Kim,[1] B. J. Kim,[2] H. Koh,[3] H. Eisaki,[4] N. P. Armitage,[5,6] and C. Kim[1]

[1]*Institute of Physics and Applied Physics, Yonsei University, Seoul, Korea*

[2]*School of Physics and Center for Strongly Correlated Materials Research, Seoul National University, Seoul, Korea*

[3]*Advanced Light Source, Lawrence Berkeley National Laboratory, Berkeley, California 94720, USA*

[4]*Advanced Industrial Science and Technology, Tsukuba, Japan*

[5]*Département de Physique de la Matière Condensée, Université de Genève, quai Ernest-Ansermet 24, CH1211 Genève 4, Switzerland*

[6]*Department of Physics and Astronomy, The Johns Hopkins University, Baltimore, Maryland 21218, USA*

(Received 28 December 2006; published 1 February 2007)

Angle-resolved photoemission spectroscopy (ARPES) data from the electron-doped cuprate superconductor $Sm_{1.86}Ce_{0.14}CuO_4$ show a much stronger pseudogap or hot-spot effect than that observed in other optimally doped *n*-type cuprates. Importantly, these effects are strong enough to drive the zone-diagonal states below the chemical potential, implying that *d*-wave superconductivity in this compound would be of the nodeless gap variety. The gross features of the Fermi surface topology and low-energy electronic structure are found to be well described by reconstruction of bands by a $\sqrt{2}\times\sqrt{2}$ order. Comparison of the ARPES and optical data from the same sample shows that the pseudogap energy observed in optical data is consistent with the interband transition energy of the model, allowing us to have a unified picture of pseudogap effects. However, the high-energy electronic structure is found to be inconsistent with such a scenario. We show that a number of these model inconsistencies can be resolved by considering a short-range ordering or inhomogeneous state.

DOI: 10.1103/PhysRevB.75.060501 PACS number(s): 74.25.Jb, 74.72.−h, 79.60.−i

In spite of their many interesting physical properties,[1–4] electron-doped high-temperature superconductors (HTSCs) have been much less studied as compared to the hole-doped HTSCs. It was not until a few years ago that high-resolution angle-resoved photoemission spectroscopy (ARPES) was applied and there are still only a handful of published papers on the subject. In their high-resolution ARPES studies, Armitage *et al.* found that for the highest-T_c samples of $Nd_{1.85}Ce_{0.15}CuO_4$ (NCCO) the near-E_F spectral weight was strongly suppressed at the momentum space positions where the underlying Fermi surface (FS) contour crosses the antiferromagnetic (AF) Brillouin zone boundary (ZB) suggesting the existence of a (π,π) scattering channel.[5] It was also found that for $(x=0.04)$ underdoped samples an electron FS pocket exists around the $(\pi,0)$ point and that at higher dopings spectral weight increases near $(\pi/2,\pi/2)$, which eventually completes the large holelike FS pocket around the (π,π) point.[6]

A possible way to view the results for the highest-T_c samples—at least qualitatively—is as a manifestation of a band reconstruction from a $\sqrt{2}\times\sqrt{2}$ static (or slowly fluctuating) spin density wave (SDW) or similar symmetry order.[7] Such a picture explains hot spots on the FS contour as due not to the opening of a pseudogap *per se* but instead to a band folding and then splitting across the AFZB, giving FS pockets around $(\pi/2,\pi/2)$ and $(\pi,0)$. Such a simple two-band interpretation enables one to understand issues such as the sign change in the Hall coefficient[8] and optical conductivity[9] spectra. However, systematic studies to test the model are lacking and there may be doubts that such a simple picture could describe the data at the level of small details.

Motivated by these issues, we have performed an extensive high-resolution ARPES study on another compound in the small family of electron-doped HTSCs, $Sm_{1.86}Ce_{0.14}CuO_4$ (SCCO), as well as optical reflection measurements. A quantitative analysis yields a number of important observations, which have implications for the gap symmetry and pairing mechanism. We find a much stronger pseudogap or "hot-spot" effect that creates a gap where a node is expected in a *d*-wave superconductor. Additionally, we find that—despite its simplicity—a SDW scenario[10] can account for various aspects of the low-energy electronic structure quite well, such as the Fermi surface topology and low-energy band dispersions. The data also clearly show the link between the optical pseudogap and the interband transition between the split bands. We argue that other anomalous aspects may be explained through the consideration of a short-range ordering or inhomogeneous state.

SCCO single crystals were grown by the traveling-solvent floating-zone method. The doping level determined by the inductive coupled plasma method was $x=0.14$. As-grown samples (unreduced) are not superconducting due to the believed presence of extra oxygen at the apical sites. Crystals were "reduced" by annealing in Ar for 48 h at 1000 °C, and then in oxygen for 24 h at 500 °C to induce superconductivity. T_c was determined to be 13 K by magnetic susceptibility measurement. ARPES experiments were performed at beamline 7.0.1 at the Advanced Light Source. 85 and 135 eV photon energies were used with a total instrumental energy and angular resolutions of approximately 50 meV and 0.4°, respectively. Additional higher-resolution data were taken at beamline 5-4 of the Stanford Synchrotron Radiation Laboratory using 16.5 eV photons with an energy resolution of 10 meV. Samples were cleaved *in situ* and laser aligned. Superior surface quality upon cleaving and small line shape differences allow us to resolve features that were not observed on related compounds. The chamber pressure was

 ©2007 The American Physical Society

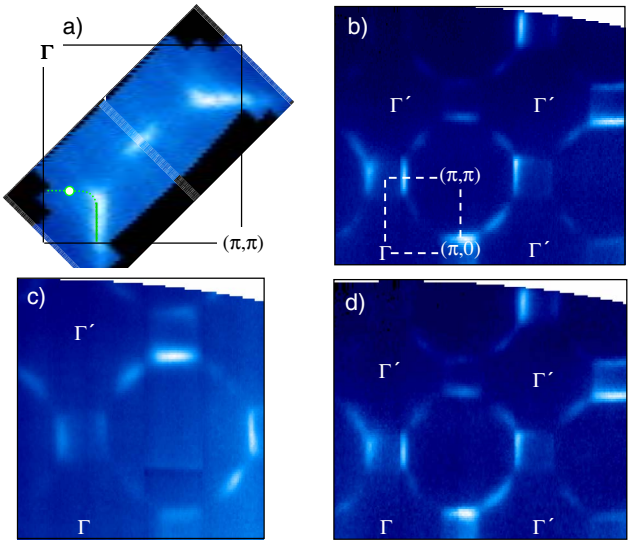

FIG. 1. (Color online) Fermi surface maps of (a) a reduced sample taken with 16.5 eV photons, (b) a reduced sample at the Sm $4d \rightarrow 4f$ edge (135 eV), and (c) an unreduced sample at 85 eV. (d) Momentum distribution plot at 100 meV binding energy. In (b), the first quadrant of the first Brillouin zone is drawn as a dashed square.

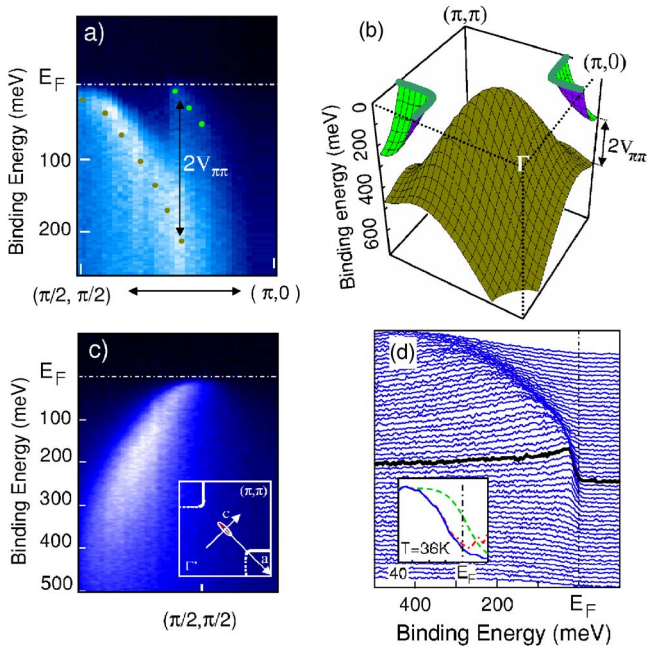

FIG. 2. (Color online) (a) Cut along the AFZB. (b) Schematic of the reconstructed band structure in the model. (c) Data along the Γ-(π,π) cut. Inset shows the FS as well as the location where data in (a) and (c) are taken. (d) Energy distribution curves (EDCs) of the data in (c). The inset shows the EDC at the E_F crossing (solid), the Au spectrum (dashed), and the EDC divided by the latter (dash-dotted).

better than 4×10^{-11} Torr and the temperature was kept between 15 and 20 K.

In Fig. 1(a), we show a spectral intensity map obtained by integrating the spectra within a 30 meV window at the Fermi energy. The photon energy is 16.5 eV. The high-intensity locus in momentum space can be interpreted as the FS. One immediately notices that the FS contour has a suppression of the spectral intensity where it crosses the AFZB $[(\pi,0)$-$(0,\pi)$ line] as observed previously for NCCO.[5] Even though such a segmented FS has been observed for other compounds, which suggests that it is an intrinsic property of the CuO planes in the electron-doped HTSCs, we performed additional experiments to make sure that all the FS segments are derived from CuO states and that our observation is not due to photoemission matrix element effects.

The FS map shown in Fig. 1(b) was taken with the photon energy tuned to the Sm $4d \rightarrow 4f$ edge (135 eV) and looks similar to the map taken with 16.5 eV photons. This excludes the possibility that any of the broken FS segments are related to Sm-derived states as its intensity would have been relatively enhanced due to the resonance effect. In addition, the FS suppression is seen in higher Brillouin zones (BZs) in which the photoemission selection rules are different from that in the first BZ. Shown in Fig. 1(c) is a similar map taken on an unreduced (nonsuperconducting) sample with 85 eV photons. Even though we were not able to obtain detailed information due to the lower resolution, the gross features of the spectra from unreduced samples are qualitatively similar to those of reduced samples. The above results confirm that the FS suppression is an intrinsic property of CuO planes in electron-doped HTSCs.

One can obtain more information by looking at the data at binding energies higher than E_F. Figure 1(d) shows the momentum distribution of the spectral intensity at 100 meV binding energy instead of at E_F. One finds that the "break" in the momentum distribution still exists at this energy and therefore the spectral weight suppression does not derive from the opening of a low-energy pseudogap at E_F but suggests that it involves energy scales of at least 100 meV. This in turn points to the scattering being of static (or quasistatic) origin.[11]

We therefore analyze our data based on a simple $\sqrt{2} \times \sqrt{2}$ SDW model band structure with characteristic wave vector (π,π). We note that, although a SDW is the natural choice based on the close proximity of the antiferromagnetic phase, our data are consistent with any ordering of characteristic wave vector (π,π). The $\sqrt{2} \times \sqrt{2}$ band structure can be obtained via simple degenerate perturbation theory by solving a 2×2 matrix, which gives

$$E_k = E_0 + 4t'(\cos k_x \cos k_y) + 2t''(\cos 2k_x + \cos 2k_y) \pm \sqrt{4t^2(\cos k_x + \cos k_y)^2 + |V_{\pi\pi}|^2} \quad (1)$$

where $V_{\pi\pi}$ is the strength of the effective (π,π) scattering, and t, t', and t'' are hopping energies. The original large FS band centered around (π,π) characterized by the three hopping energies t, t', and t'' reconstructs due to the (π,π) scattering and splits into two bands. We analyze the data quantitatively within this model.

The best way to view the band splitting is to look at the data along the AFZB as the splitting along this cut should show a constant value of $2V_{\pi\pi}$ within the model. Figure 2(a) shows the data along the AFZB taken with 16.5 eV photons.

One can see two bands with a roughly constant splitting, consistent with the model and theoretical results.[12] We note that this observation clearly contradicts the recent claim of anisotropic spin correlation gap.[14] One also sees that, unlike recent data on NCCO, there are no quasiparticlelike peaks or even FS crossing in the hot spot itself.[13] Fitting of the experimental dispersion in Fig. 2(a) as well as the FSs in Fig. 1 within the model gives us $t=0.25$ eV, $t'=0.036$ eV, $t''=0.027$ eV, and $V_{\pi\pi}=0.11$ eV. The band structure constructed with the extracted parameters is depicted in Fig. 2(b). We see that the lower of the split bands may contribute to a small holelike FS pocket near $(\pi/2,\pi/2)$ if it crosses E_F, while the upper one gives an electronlike FS centered at $(\pi,0)$. We note that the observed $V_{\pi\pi}$ value is larger than the analogous one in NCCO.[5]

As shown in Fig. 2(b), although the model predicts that band folding should occur across the AFZB, such folding has not been observed in the published data to date. Our data along the Γ to (π,π) cut shown in Fig. 2(c) shows such a band folding as we go from Γ to (π,π), the band approaches E_F, bends at around 50 meV, and appears to fold back near $(\pi/2,\pi/2)$. This is clearly seen in the energy distribution curves (EDCs) of the same data in Fig. 2(d). We attribute the observance of band folding in SCCO to the better quality of the data and a larger $V_{\pi\pi}$. The quasiparticlelike sharp peak was comparatively smaller in the case of NCCO with a width approximately double.[15] This appears to indicate a better surface quality for SCCO.

The $\sqrt{2}\times\sqrt{2}$ band model also allows one to explain the peculiar straight section of the FS near $(\pi,0)$ as deriving from the original curved FS contour being straightened due to the band reconstruction. This would be very hard to understand if the break in the FS contour were due to a simple suppression of the FS in a single band. In addition, fitting of the FS by a single contour and counting the electrons in the occupied k-space region gives a FS volume of 1.07 ± 0.01 which is smaller than the expected value of 1.14 (14% doping); whereas the FS volume measured based on the two-band model depicted in Fig. 2(b) is 1.13 ± 0.01 (the difference mostly coming from the nodal segment being completely occupied) which is reasonably close to the doping.

The inset to Fig. 2(d) shows a comparison of both raw data and data divided by the Fermi function at the E_F crossing taken at $T=36$ K, well above the T_c. The spectra clearly show that the lower band never quite reaches E_F and there is in fact no FS pocket near the $(\pi/2,\pi/2)$ point. Therefore, the "FS" segment near $(\pi/2,\pi/2)$ in Fig. 1(a) is due to the finite size of the energy integration window. We indeed find that the relative intensity of the FS near $(\pi/2,\pi/2)$ quickly drops in comparison to the other as we reduce the size of the integration window. In SCCO the $V_{\pi\pi}$ is sufficiently large to push the FS folded bands below E_F along the zone diagonal. Recently, there have been conflicting reports on the gap symmetry determined by magnetic penetration depth measurements.[16,17] If—as in other n-type cuprates—superconducting SCCO at this doping level is d wave,[13,18,19] our result directly shows that a "nodeless gap" can be compatible with d-wave symmetry and provides a clue to the gap

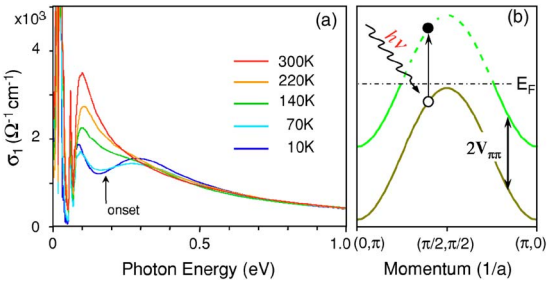

FIG. 3. (Color online) Real part of the conductivity at different temperatures obtained by reflectivity measurements. The arrow indicates the onset of the interband transition. The panel on the right is a schematic of the band structure and interband transition along the AFZB.

symmetry controversies. To our knowledge, this is the first momentum-resolved experimental evidence for a nodeless d-wave gap with a gap only near $(\pi,0)$ and no low-energy zone-diagonal states.

Pseudogap effects are also seen in optical measurements[20] and connection to the pseudogap in SDW model has been proposed.[9] However, a clear experimental connection between the two on the same system has previously not been obtained to our knowledge. As the upper band is partially filled, interband transitions between the two band sheets are possible, which can be confirmed by optical measurements. Shown in Fig. 3 is the optical conductivity at different temperatures obtained by reflectivity measurements. In the 10 K spectrum, one can see a peak near 300 meV with an onset near 200 meV. This is compatible with the interband transition inferred from the ARPES of $2V_{\pi\pi}=220$ meV and allows us to interpret the two phenomena (pseudogaps in ARPES and optical measurements) in a unified picture. As the temperature increases, the interband transition peak weakens, implying weakening of the $\sqrt{2}\times\sqrt{2}$ reconstruction. Note, however, that the energy position of the peak remains more or less the same. Similar but weaker features have been observed in other compounds and referred to as a pseudogap.[9,20] We also note that the fact that the onset energy in $x=0.15$ NCCO is smaller than that of SCCO is compatible with the fact that NCCO has a smaller $V_{\pi\pi}$. Considering the fact that SCCO has lower optimal T_c, the pseudogap appears to have an anticorrelation with $T_c^{optimal}$.

Even though the simple SDW model explains various aspects of the electronic structure in electron-doped HTSCs, there are important aspects with which it is not compatible. Figures 4(a) through 4(d) show various cuts as marked in Fig. 4(f). These data are similar to other recent ones on NCCO.[14] From the fact that the minimum splitting between the upper and lower SDW bands appears to change with momentum, an anisotropic SDW gap was argued for.[14] However, in such a case, the two bands should still backfold symmetrically across the AFZB, unlike the observed results. Here it can been seen that, while the upper band more or less ends exactly at the AFZB, the lower one clearly overshoots the AFZB, which is incompatible with an ordering vector (π,π). Instead, the lower one is more reminiscent of the original unreconstructed band. This aspect of the data has been previously overlooked.

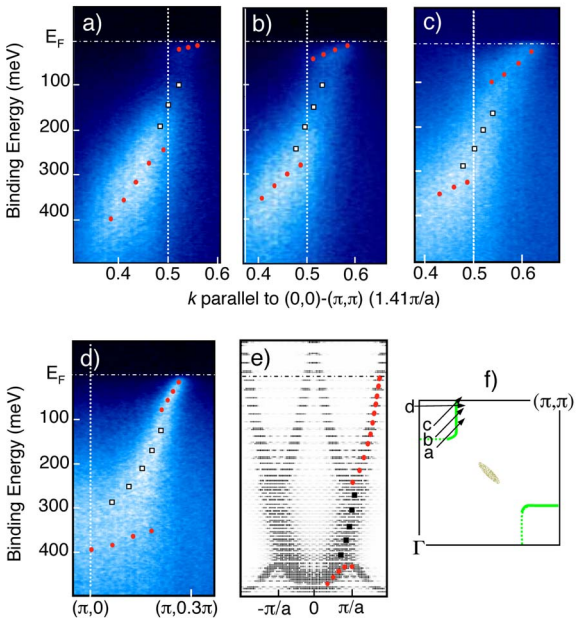

FIG. 4. (Color online) ARPES data in (a) through (d) are taken along the cuts marked in (f). (e) Eigensolutions based on numerical model detailed in text, which mimics a short-range ordered state. Squares correspond to the original band and the circles to the reconstructed one.

The observed discrepancy between the data and model could be attributed to existence of short-range ordering or an inhomogeneous magnetic state. To illustrate the effect of a short-range ordering, we consider one-dimensional electrons that are subject to short-range periodic potentials of strength $V_{\pi\pi}$ and periodicity a. Energy eigenvalue solutions are obtained for potentials with various extents and plotted in Fig. 4(e). This simulates a situation where electrons experience only a short-range order. One notes that it gives not only the folded bands (red circles) but also the original band (black squares). In this interpretation, the middle band in Fig. 4(a)–4(d) represents the original band which disperses uninterrupted through the AFZB. In fact, while recent neutron scattering results show that a long-range AF order cannot coexist with superconductivity,[21] a short-range AF order exists at low temperature[4] in NCCO. If the short-range $\sqrt{2} \times \sqrt{2}$ ordering is indeed from AF fluctuations, the temperature dependence of the optical spectrum is naturally explained. At a very low temperature, the two bands are relatively well defined and so is the interband transition peak. As the temperature is raised, the AF coherence length gets shorter and the two bands become ill defined. As a consequence, the interband transition peak becomes weaker, resulting in a filling of the pseudogap. This naturally connects the AF energy scale with that of the pseudogap formation. It is important to note in this picture that it is not the energy scale $V_{\pi\pi}$ but the ordering length that changes. Therefore, the pseudogap does not close but instead fills in as the temperature increases. Alternatively, the observed ARPES spectra can be explained in terms of an energy scale where features below about 100 meV derive from reconstructed bands and above 100 meV from the original band. These observations can be explained with a (π, π) scattering which becomes ineffective above a certain energy scale (not necessarily momentum dependent). A similar "ineffectiveness" may have been observed in the checkerboard pattern measured by scanning tunneling microscopy on $(Na,Ca)_2CuO_2Cl_2$ which disappears for ω above 50 meV.[22]

Finally, another discrepancy between the data and the simple model is in the intensity of the folded band. One can obtain the expected relative intensities of the folded bands from the eigensolution of the 2×2 matrix equation. Even though band folding is clearly observed as shown in Fig. 2, the intensity appears weaker than predicted within the model. For example, the intensity of the folded band at the k point marked by a green circle in Fig. 1(a) should be about 1/4 of the intensity at the cross, but is observed to be much weaker. This observation is independent of the photon energies or Brillouin zone, thus showing it is not due to the matrix element effect. This aspect of the data should be described by a more rigorous theory. Interestingly, many-body calculations based on the Hubbard model, which show the existence of a short-range ordering, exhibit a weakened intensity of the folded bands.[23]

The authors thank T. Tohyama, A. M. Tremblay, and J. H. Han for helpful discussions and D. H. Lu for technical assistance. This work is supported (in part) by KOSEF through CSCMR. N.P.A. is supported by the NSF IRF Program and MaNEP. ALS and SSRL are operated by the DOE's Office of BES.

[1] Z. Z. Wang *et al.*, Phys. Rev. B **43**, 3020 (1991).
[2] Y. Dagan *et al.*, Phys. Rev. Lett. **92**, 167001 (2004).
[3] M. Matsuda *et al.*, Phys. Rev. B **66**, 172509 (2002).
[4] K. Yamada *et al.*, Phys. Rev. Lett. **90**, 137004 (2003).
[5] N. P. Armitage *et al.*, Phys. Rev. Lett. **88**, 257001 (2002).
[6] N. P. Armitage *et al.*, Phys. Rev. Lett. **87**, 147003 (2001).
[7] N. P. Armitage, Ph.D. thesis, Stanford University, 2001.
[8] J. Lin and A. J. Millis, Phys. Rev. B **72**, 214506 (2005).
[9] A. Zimmers *et al.*, Europhys. Lett. **70**, 225 (2005).
[10] We do not necessarily suggest spin origin. Any $\sqrt{2} \times \sqrt{2}$ static ordering would produce similar results.
[11] F. Onufrieva and P. Pfeuty, Phys. Rev. Lett. **95**, 207003 (2005).
[12] T. Tohyama, Phys. Rev. B **70**, 174517 (2004).
[13] H. Matsui *et al.*, Phys. Rev. Lett. **95**, 017003 (2005).
[14] H. Matsui *et al.*, Phys. Rev. Lett. **94**, 047005 (2005).
[15] N. P. Armitage *et al.*, Phys. Rev. B **68**, 064517 (2003).
[16] M. S. Kim *et al.*, Phys. Rev. Lett. **91**, 087001 (2003).
[17] A. Snezhko *et al.*, Phys. Rev. Lett. **92**, 157005 (2004).
[18] N. P. Armitage *et al.*, Phys. Rev. Lett. **86**, 1126 (2001).
[19] C. C. Tsuei and J. R. Kirtley, Phys. Rev. Lett. **85**, 182 (2000).
[20] Y. Onose *et al.*, Phys. Rev. Lett. **87**, 217001 (2001).
[21] E. Motoyama *et al.* (unpublished).
[22] T. Hanaguri *et al.*, Nature (London) **403**, 1001 (2004).
[23] D. Sénéchal and A. M. S. Tremblay, Phys. Rev. Lett. **92**, 126401 (2004).